The effects of magnetic surface stress on electrospray of an ionic liquid ferrofluid

Kurt J. Terhune* and Lyon B. King†
Michigan Technological University, Houghton, MI, 49931

Benjamin D. Prince‡
Air Force Research Laboratory, Kirtland AFB

Nirmesh Jain§ and Brian S. Hawkett**
The University of Sydney, NSW 2006, Australia

Four solutions of an ionic liquid ferrofluid (ILFF) using 1-ethyl-3-methylimidazolium bis(trifluoromethylsulfonyl)imide (EMIM-NTf2) as the carrier liquid were emitted from a capillary electrospray source and its beam was measured using a time-of-flight mass spectrometer (TOF-MS) and a downstream stack of Faraday plates. The solutions had 3.04, 5.98, 8.80, and 14.15 wt% iron-oxide nanoparticles making them susceptible to magnetic fields. A Helmholtz coil was used to impose a magnetic stress onto the electrospray source. The addition of nanoparticles to neat IL increased viscosity, and decreased conductivity and surface tension of the fluid. The emission current followed the proportionality $I \sim \sqrt{Q\gamma K}$, with a slope that depended upon both the concentration of nanoparticles and the magnetic field. The addition of nanoparticles caused an increase in the total emission current from the source when compared to neat IL running at the same flowrate. Conversely, the addition of a magnetic stress decreased the total emission current from the source compared to the field-free case; the change was larger in solutions with a higher wt% of nanoparticles. The magnetic stress also decreased the minimum stable flowrate that could be achieved, widening the operational envelope beyond that of traditional non-magnetic electrospray.

Nomenclature

e	=	Elementary charge
ε_0	=	Permittivity of free space
ε	=	Permittivity
E	=	Particle kinetic energy
$F(\varepsilon)$	=	F. de la Mora's factor for electrosprays
γ	=	Interfacial surface tension
H	=	Magnetic field
I	=	Emission current
K	=	Conductivity
L_c	=	Length of capillary tube
L_{TOF}	=	Length of time-of-flight tube
m	=	Particle mass
m/q	=	Particle mass-to-charge ratio
M	=	Magnetization
μ_0	=	Magnetic permeability of free space

* Graduate Research Assistant, Mechanical Engineering-Engineering Mechanics, 815 RL Smith Building, 1400 Townsend Drive. AIAA Student Member
† Professor, Mechanical Engineering-Engineering Mechanics, 1014 RL Smith Building, 1400 Townsend Drive. AIAA Member
‡ Research Chemist, Space Vehicles Directorate, 3550 Aberdeen Ave SE, Building 570. AIAA Member
§ Research Associate, School of Chemistry and Key Centre for Polymers and Colloids, Chemistry F11
** Associate Professor, School of Chemistry and Key Centre for Polymers and Colloids, Chemistry F11

η = Liquid viscosity
ΔP = Pressure drop through capillary tube
q = Particle charge
Q = Volumetric flowrate
$Q_{\min}$ = Minimum volumetric flowrate
r_c = Capillary tube radius
t_{flight} = Time-of-flight
u = Particle velocity
V = Voltage

I. Introduction

APPLYING a strong electrostatic stress to the interface of a conductive or dielectric liquid creates an instability in the surface. If the stress is sufficiently large to balance the counteracting surface tension the liquid forms a conical protrusion called a Taylor cone; if the electrostatic stress is increased to overcome surface tension it will begin to emit a jet and fine aerosol spray (Figure 1).[1] The process of emitting the liquid in this manner is called electrospraying and is used in many applications including electrospray ionization for mass spectrometry,[2-7] electrospinning,[8,9] particle deposition,[10-12] and colloid thrusters.[13-16]

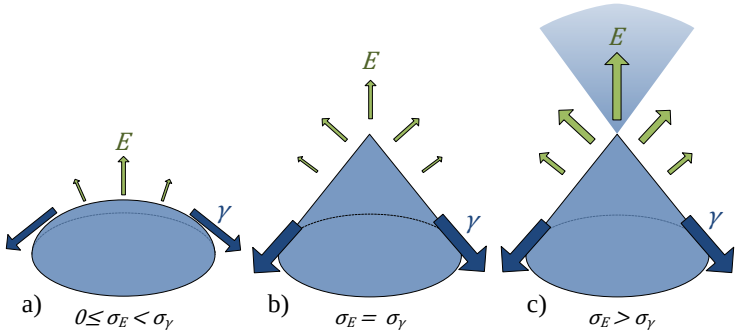

Figure 1. A droplet of ionic liquid under an electrostatic stress that (a) is zero or nonzero but less than the interfacial surface tension, (b) is balanced by the interfacial surface tension forming a Taylor cone, and (c) has overcome the interfacial surface tension and begun electrospraying.

Empirical findings have shown that the emitted current from an electrospray source is a function of the propellant flowrate, electrical conductivity, surface tension, and electrical permittivity as described by Eq. 1.[18,19]

$$I = F(\varepsilon)\sqrt{\gamma K Q / \varepsilon} \tag{1}$$

These relationships apply to many sprayable liquids including a class used predominately in colloid thrusters called ionic liquids (ILs). ILs are room-temperature liquid salts and are desired because they can be comprised of a multitude of different anion-and-cation combinations which can vary the liquid properties for a given application.[17-19]

Beginning in 2013 researchers began using IL ferrofluids (ILFF) as electrospray propellants.[20,21] ILFFs are produced by adding nanometer-scale ferromagnetic particles coated in a surfactant to ILs. The size of the particles, roughly 30 nm in diameter, allows them to remain in suspension through Brownian motion; the surfactant prohibits clumping of particles which would cause them to precipitate out of the fluid. The end product is a superparamagnetic conductive fluid.

Applying a magnetic field to an ILFF that is being electrosprayed changes the behavior of the spray. Specifically, the additional magnetic surface stress was observed to elongate the fluid in the direction of the field (illustrated in Fig. 2),[20-22] and reduce the onset voltage of electrospray.[23] A theoretical study on the potential energy of bulk fields (gravity, surface tension, magnetic and electric) imposed on a pool of magnetic fluid (ferroelectrohydrodynamics) concluded that the combined fields change the conditions of operation.[24]

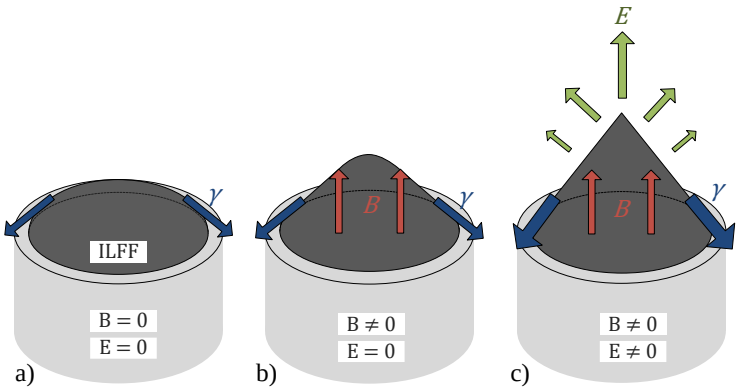

Figure 2. Ionic liquid ferrofluid at a capillary outlet under (a) interfacial surface tension, (b) interfacial surface tension and a magnetic field in balance elongating the liquid meniscus, (c) interfacial surface tension, magnetic field, and electric field in balance at the onset of emission.

Because the combined magneto-electrospray was only recently demonstrated there exists no description of how the magnetic effects combine with the electric effects to produce spray. Fortunately, due to the prominence of ILs in capillary electrospray research the relationship between emission current, propellant flow rate, and the electric field has been well documented using multiple IL propellants in capillary systems.[4,5,14,19,25-27] Thus a capillary electrospray system is an ideal configuration to isolate any new effects imposed by the addition of nanoparticles and applied magnetic field. This paper presents a first effort to document the effect of magnetic stress on a high-conductivity, ferrofluid capillary electrospray.

II. Goal of Study

Pressure-fed capillary electrospray sources have been widely studied and their behavior is well documented.[4,5,14,22,28-30] Our approach was to isolate effects due to the colloidal nanoparticles and magnetic stress by examining a conventional capillary electrospray system operating using varying solutions of nanoparticles in the ILFF with and without a magnetic field and comparing these cases against well-established baselines. The goals of the research presented in this paper were to (1) analyze the effect colloidal nanoparticles have on the operational range (emission current and flowrate) of a capillary electrospray, and (2) analyze the effects of an applied gradient-free magnetic field on the operational range (emission current and flowrate) of an ILFF capillary electrospray.

III. Background

A. Ferrofluids

The magnetic nanoparticles that form a ferrofluid maintain their stable colloidal nature due to their small size and the polymer surfactant which coats them. The selection of the surfactant is dependent on the material and surface structure of the nanoparticles, along with the surfactant's affinity with the carrier liquid. Many materials have been used to provide particle stabilization,[28-30] but a standard surfactant has both a polar adsorbent which anchors to the nanoparticle and a non-polar tail which is soluble in the carrier liquid. The dispersant chosen to stabilize the magnetic particles in the ionic liquid EMIM-NTf2 is a block copolymer 10MAEP-60DMAM, which is comprised of 10 poly(monoacryloxyethyl phosphate) (PMP) blocks, a RAFT end group ($CS_3C_4H_9$), 60 poly(N,N-dimethylacrylamide) (PDA) blocks, and a functionalizing group ($CH_3CHCOOH$). The former two parts of the molecule make up the absorbent anchor, and the latter two are the soluble stabilizers which provide steric stabilization. The process to synthesize the ILFF is described by Jain et al.[28] and King et al.[22]

B. Ionic Liquid Ferrofluid Electrosprays

Two forms of ILFF electrosprays have been studied – electrospray from a "needle-free" ILFF peak formed by the Rosensweig instability, and electrospray from a capillary needle with and without an applied magnetic field.[31] Electrosprays from the Rosensweig instability have been produced from a single peak,[22,23,32] and an array of five peaks.[20-22] In each of these electrospray studies, dark residue on the extraction electrode revealed evidence of the magnetic nanoparticles. Madden et al. also observed that the addition of a magnetic field extends the stability range of flowrates, currents, and voltages for ILFF electrosprays which theoretically enables the production of smaller droplets.[31]

C. Mass Spectrometry of Electrospray Propulsion Systems

Mass spectrometry is a standard method of analyzing the emission of electrospray thrusters to predict their performance in space propulsion applications.[2,5,27,33-35] A mass spectrometer can measure the value of m/q for species emitted from these thrusters. A quantitative understanding of the m/q of an electrospray thruster is paramount in designing them for specific missions. It can determine whether it can be used in a high thrust-to-power mission or a high Isp mission, or instead provides variable m/q to satisfy both types of missions.

An orthogonal extraction TOF mass spectrometer pulses an extraction/acceleration electrode (V_i) placed perpendicular to the axis of the electrospray beam to capture a volume of the beam and accelerate it, with a narrow kinetic energy range, toward a charge-exchange multiplier (CEM). The difference in time of the initial pulse and the time of the signals gathered by the CEM are used to determine the flight time of the various particles in the volume of the electrospray beam, under the assumption that all particles have approximately the same kinetic energy once extracted. The time-of-flight of the particles can be directly related to their mass-to-charge ratios (m/q) through the relationship between the electrical and kinetic energy of the particles, Equation 2.

$$\frac{1}{2}mu^2 = qeV \tag{2}$$

Rearranging Equation 2 for mass-to-charge results in $\frac{m}{q} = \frac{2V}{u^2}$. Substituting the length of the TOF chamber (L_{TOF}) divided by the time-of-flight (t_{flight}) for the velocity and solving for m/q, one derives a relationship for the mass-to-charge ratio of the particles based on their flight time through the TOF chamber, Eq. 3.

$$\frac{m}{q} = \frac{L_{TOF}^2}{t_{flight}^2 2V} \tag{3}$$

IV. Experimental Facility and Methods

A. Time-of-flight Mass Spectrometer Facility

The TOF-MS system housed at the AFRL is fully described elsewhere.[36], thus the following is a brief description of the system. The orthogonal reflectron TOF-MS can detect particles in the range of a few amu/e to over 1,000,000 amu/e. The facility is a 1-meter long by 0.254-meter wide by 0.254-meter tall reflectron flight-tube detection chamber that is situated orthogonal to a 0.5-meter long source chamber. A multichannel plate (MCP) is used as the detector and is positioned at both ends of the reflectron flight-tube to provide both linear and reflectron TOF measurements. The apparatus has been described in detail by The source chamber is maintained at a pressure of 10^{-7} Torr, while the detection chamber is maintained at approximately 2 x 10^{-8} Torr. The pressures are achieved using two 250 l/s turbo-molecular pumps backed by one 600 l/min dry scroll pump.

When using the TOF-MS to collect mass spectra multiple lenses, grids and deflectors, were attached at the end of the source (discussed in section IV-E of Terhune et al.[37]) which are used to maximize the beam intensity entering the TOF pulsing region. The pulsing region consists of a pair of parallel plates which are parallel to, but offset from, the beam axis. Each plate has a gridded aperture to allow orthogonal transmission of ion species when the voltages on the plates are pulsed. Continuing along the original beam axis, a quartz crystal microbalance (QCM), used to quantify the mass flow rate, and a Faraday cup, used to measure the current of the beam, are located after a 6 mm rectangular aperture at the end of the parallel plates.

In experiments measuring the emission current from the beam, a set of three Faraday plates were attached to the source, located 28.6, 41.75, and 54.9 mm from the extractor. The two plates located at 28.6 and 41.75 mm from the extractor had apertures of 12.69 and 19 mm, respectively. Simultaneous measurement of the current from each plate provides a measure of beam divergence of the electrospray.

B. Capillary Electrospray Source

The capillary electrospray source, shown in Figure3 a., produced the electrospray beams analyzed in the TOF-MS facility. The source is comprised of (1) an extractor plate which has a 1-mm-diameter aperture, (2) 0.50-m or 0.75-m long, 75-μm-inner diameter capillary needle, with a wall thickness of ~5 μm at the needle apex, (3) a PTFE block to both hold and isolate the needle, and (4) set screws to align the needle with the extractor aperture. The IL or ILFF was fed to the capillary needle by pressurizing a vial of liquid outside the vacuum facility. A set pressure, p_0, was accomplished by opening or closing valves which either fed nitrogen gas into the vial or removed gas from the vial via a mechanical scroll pump. The liquid was electrically biased via an electrode inserted into the vial. The feed system is shown in Figure 3 b. The flowrate of the liquid being fed to the capillary source was determined via the bubble

method, wherein the velocity of a bubble introduced in the feedline was measured for a given vial pressure. The velocity was then converted to volumetric flowrate using the known dimensions of the capillary tube.

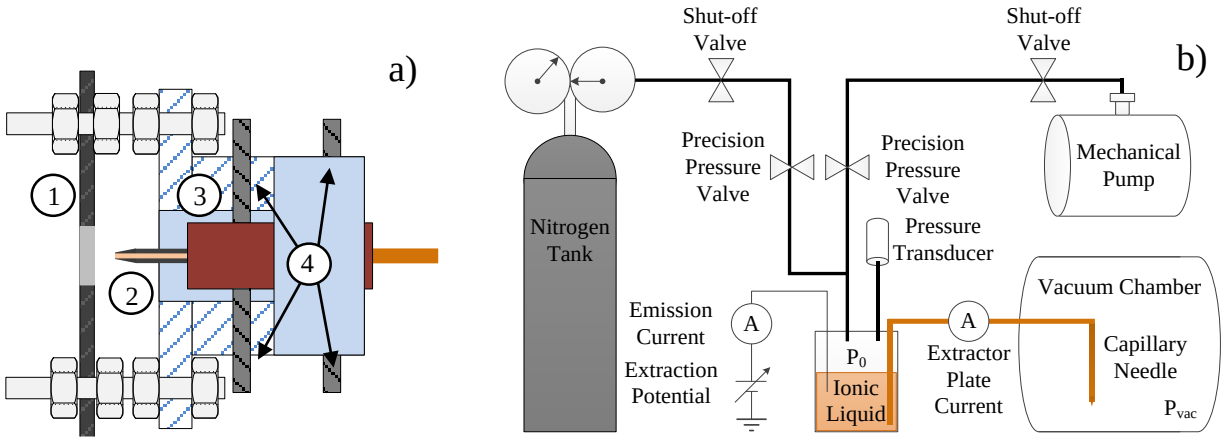

Figure 3. (a) Capillary electrospray source comprised of (1) extractor plate, (2) capillary needle, (3) PTFE isolation block, (4) alignment set screws. (b) Schematic of the capillary source pressure feed system.

C. Electrospray Fluids

Five fluids were used throughout the various experiments reported in Section V. They are the neat IL EMIM-NTf2, and four solutions of EMIM-NTf2 ferrofluid with varying concentration of magnetic nanoparticles. The ferrofluids will henceforth be called ILFF-10, ILFF-20, ILFF-30, and ILFF-50 based on the volume percent of a concentrated parent ILFF that was mixed with neat IL. The parent ILFF contained 26.0 wt% iron oxide nanoparticles which led to nanoparticle concentrations in the four solutions of 3.04, 5.98, 8.80, 14.15 wt% for ILFF-10, ILFF-20, ILFF-30, and ILFF-50, respectively. The volumes of neat IL and ILFF, and nanoparticle concentrations that comprised each ILFF solution are tabulated in Table 1.

Table 1. Diluted ILFF Solutions used in the TOF-MS experiments.

ILFF Dilution	Volume neat IL (mL)	Volume ILFF (mL)	Total Volume (mL)	Nanoparticle Concentration (% wt/wt)	Density (g/ml)
Neat IL	NA	NA	NA	0.00	1.523
ILFF-10	0.18	0.02	0.2	3.04	1.55
ILFF-20	0.16	0.04	0.2	5.98	1.58
ILFF-30	0.14	0.06	0.2	8.80	1.61
ILFF-50	0.10	0.10	0.2	14.15	1.64
Parent ILFF	NA	NA	NA	26.00	1.815

D. Magnetic Field

A Helmholtz coil provided a variable magnetic field that could be applied to the source for several minutes at a time. The solenoid design was chosen to provide a gradient free field thus removing the effect of a Kelvin force, Equation 4, at the emission site.

$$\text{Kelvin force density} = \mu_0 M \nabla H \tag{4}$$

The Helmholtz coil consist of two 19-cm-diameter, 500-wrap coils separated by a distance of 10 cm. The coils required cooling to prevent the radiative heat from affecting the operation of the electrospray source; two methods were used: a water-cooled jacket lining the center wall of the coils, and forced air convection using a box fan. The Helmholtz coil assembly was concentrically aligned over the exterior of the source vacuum envelope using set screws. Figure 4 shows the Helmholtz coil assembly attached to the source flange of the TOF chamber.

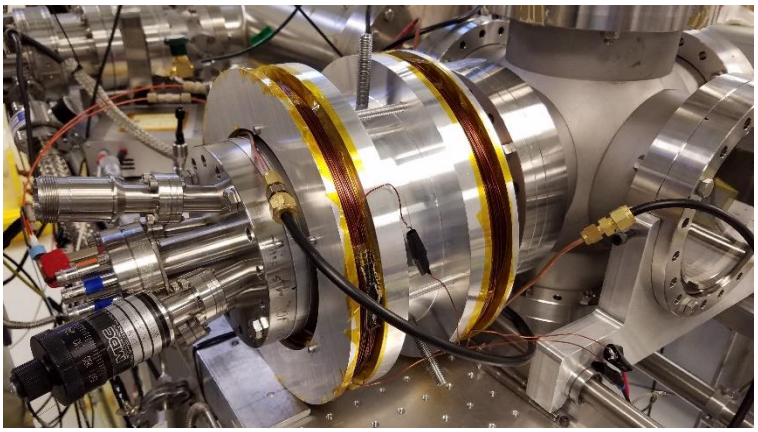

Figure 4. Helmholtz coil assembly attached to the source flange of the TOF-MS facility. The Helmholtz coil was capable of producing 200 Gauss at 5 Amps.

E. Experimental Methods

We conducted two experiments and one control in this research: (Exp-1) emission and extractor current measurement of a capillary source operating on three ILFF solutions, ILFF-10, ILFF-20, ILFF-30, with and without an applied magnetic field. (Exp-2) minimum flowrate determination of the capillary source using three ILFF solutions, ILFF-10, ILFF-30, and ILFF-50, with and without an applied magnetic field, (Exp-C) control experiments measuring the emission current and minimum flowrate of a neat IL electrospray with and without an applied magnetic field.

The feed system configuration of the electrospray source used in the three experiments differed, specifically between the two parts of Exp-C. The feed system configuration used in part 1 had a total capillary length of 0.73 m, and a 3-way inline capillary valve. For Exp-1, Exp-2 and part 2 of Exp-C, a modified feed system configuration was used which reduced the overall capillary length to 0.50 m and eliminated the inline valve to prevent any potential clogging issues when running the ILFF.

In Exp-1 the source was inserted into the TOF-MS facility and operated on the ILFF-10 solution at 0.52, 0.78, 1.04 nl/s with the liquid reservoir biased to 900 V and the extractor plate biased to -900 or -950 V to establish a working electrospray. Emission current and extractor currents were recorded for each flowrate. The process was repeated for the capillary source running on ILFF-20 and ILFF-30 solutions at the respective flowrates and extraction voltages (liquid reservoir always biased to 900V) for each solution, listed in Table 2. A 200-Gauss magnetic field was applied to the source, while maintaining the same flowrate and extraction voltage used when no magnetic field was applied, and the emission and extractor currents were recorded for each flowrate.

In Exp-2 the source was inserted into the TOF-MS facility and operated at the lowest flowrate for ILFF-10 completed in Exp-1 (see Table 2) with the liquid reservoir biased to 900 V and the extractor plate biased to -700 V. Once the electrospray emission stabilized the vial pressure was decreased at a rate of approximately 0.5 Torr-per-second until the emission became erratic or extinguished. Mass spectra of the electrospray operating at the established minimum flowrate were then collected. A 200-Gauss magnetic field was applied to the electrospray and the same procedure was followed to establish the minimum flowrate. Once established a mass spectra scan of the electrospray was collected. This procedure was repeated for ILFF-30 and ILFF-50 solutions.

Further minimum flowrate measurements in Exp-2 were completed following a rebuild of the capillary source. Determining the minimum flowrate followed the same procedure to produce electrospray. However, only the telemetry of the pressure, emission current, extractor current, and the current collected from the three Faraday plates (which were input into a DAQ system) were recorded; using the Faraday plate stack made it inherently impossible to collect mass spectra. Furthermore, at least three different potentials between -1500 V to -2000 V were used as the extraction voltage, the lower bound was set as the closest 100V step above emission shutoff.

For part 1 of Exp-C the source was operated at five vial pressures while the magnetic field strength was ramped from zero Gauss to 200 Gauss and back to zero Gauss in approximately 30 seconds. The emission current and magnetic field strength were recorded using a DAQ system. We did not determine the flowrates for these tests using the bubble method, however, we estimated them to be 0.27, 0.41, 0.54, 0.68, 0.82, 1.09 nl/s for 50, 75, 100, 125, 150, and 200 Torr, respectively, using the Poiseuille-Hagen flow equation.

For part 2 of Exp-C the electrospray source operated at three flowrates: 0.63, 0.95, and 1.26 nl/s using the modified source configuration (to provide direct comparison to ILFF Exp-1), while measuring the emission current

and extractor current. Once the electrospray was established the vial pressure was decreased at a rate of approximately 0.5 Torr-per-second until the emission became erratic or extinguished. Mass spectra of the electrospray operating at the established minimum flowrate were then collected. A 200-Gauss magnetic field was applied to the electrospray and the same procedure was followed to establish the minimum flowrate.

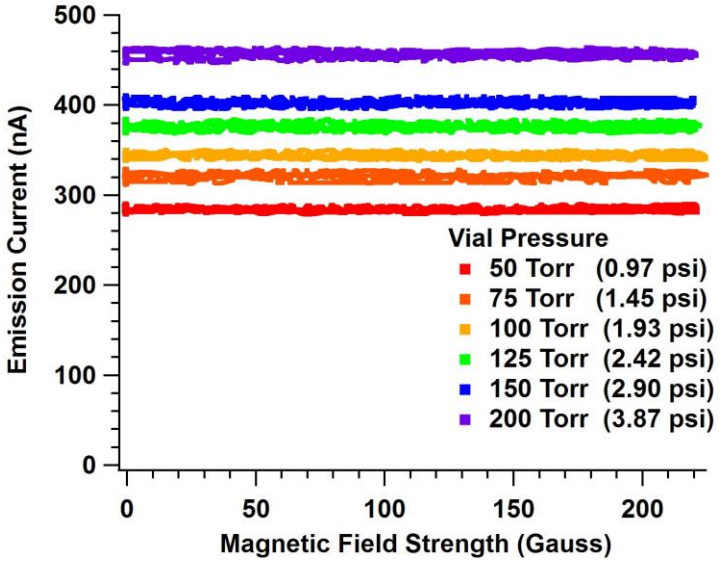

Figure 5. Emission current plotted against magnetic field strength curves of a neat IL electrospray operating at five vial pressures (flowrates) of neat IL. Extraction voltage was -1750 V.

V. Results

A. Electrospray Source Operating Characteristics

Part 1 of Exp-C showed that the applied magnetic field had no significant effect on the emission current of a neat IL electrospray (Figure 5.). The emission current varied from -283 nA for 0.27 nl/s up to -457 nA for 1.09 nl/s and was constant for each flowrate while subjected to the magnetic field. Results from Exp-C, part 2 were the emission and extractor plate currents, and extraction voltages of neat IL electrospray emission in zero magnetic field, shown in Table 2. The results are compared to the results of the emission and extractor plate currents of ILFF solutions electrosprays in section VI. A magnetic field was not applied in part 2, therefore emission and extractor currents were not measured for the neat IL subjected to the 200-Gauss magnetic field; part 1 proved that the magnetic field had no effect on the emission and alleviated the necessity to duplicate the measurement.

Operating the capillary source using the ferrofluids, with and without the applied magnetic field, resulted in several changes in the spray when compared to the neat IL. First and foremost, the addition of the nanoparticles changed the IL fluid properties of viscosity, surface tension and electrical conductivity, which, consequently, changed the magnitude of the emission current, extractor current, and downstream current measured on the Faraday plates. Throughout the testing the emission current and extractor currents were recorded. They are tabulated in Table 2.

Table 2. Average emission and extractor plate currents measured from the electrospray source operating on the neat IL and three solutions of ILFF, with and without an applied magnetic field. The extraction voltage is also provided. The neat IL electrospray was not subjected to a magnetic field in the modified source configuration.

ILFF Solution	Vial Pressure (Torr)	Flowrate (nl/s)	Mean Emission Current (nA)	Mean Extractor Plate Current (nA)	Mean Emission Current (nA)	Mean Extractor Plate Current (nA)	Extraction Voltage (V)
			0 Gauss		200 Gauss		
Neat IL	100	0.63	-472.5	61.22	N/Meas.	N/Meas.	-1800 V
	150	0.95	-562.50	116.11	N/Meas.	N/Meas.	-1800 V
	200	1.26	-630.00	337.78	N/Meas.	N/Meas.	-1800 V
ILFF-10	100	0.52	-455.50	195.53	-433.93	200.48	-1800 V
	150	0.78	-550.31	277.91	-539.72	268.34	-1850 V
	200	1.04	-666.13	395.83	-667.50	395.25	-1850 V
ILFF-20	100	0.47	-504.14	202.40	-462.66	201.88	-1750 V
	150	0.71	-608.91	335.31	-590.63	350.97	-1850 V
	200	0.94	-771.25	490.83	-719.38	462.10	-1850 V
ILFF-30	150	0.54	-727.73	298.99	-660.09	264.68	-1700 V
	200	0.72	-822.66	378.55	-735.47	319.57	-1700 V
	250	0.9	-1074.23	736.12	-947.813	665.00	-1750 V

B. Minimum Flowrate

Results from the minimum flowrate experiment are tabulated in Table 3. Minimum flowrates for stable electrospray operation were determined for four fluids, neat IL, and ILFF-10, ILFF-30 and ILFF-50 solutions at multiple extraction voltages. The minimum flowrates for an electrospray running on the four fluids while being subjected to a 200-Gauss magnetic field were determined for the same extraction voltages and are also in Table 3. The needle clogged during testing, and the source was rebuilt; the needle-to-extractor distance changed as a result of the re-build which required an adjustment in extraction voltage to maintain a stable electrospray.

Table 3. Minimum flowrates for stable electrospray operation using four fluids under the two cases of zero applied magnetic field and a 200-Gauss applied magnetic field. The extraction voltage required for operation is also included.

Fluid	Minimum Flowrate (nl/s)		Extraction Voltage (V)
	0 Gauss	200 Gauss	
Neat IL	0.19	0.19	-1500
ILFF-10	0.31	0.26	-1500
ILFF-10	0.231	0.225	-1500
ILFF-10	0.237	0.239	-1600
ILFF-10	0.238	0.250	-1700
ILFF-10	0.274	0.270	-1800
ILFF-30	0.52	0.41	-1500
ILFF-30	0.308	0.312	-1600
ILFF-30	0.428	0.378	-1700
ILFF-30	0.506	0.405	-1800
ILFF-50	0.4	0.26	-1600
ILFF-50	0.398	0.322	-1800
ILFF-50	0.403	0.308	-1900
ILFF-50	0.387	0.288	-2000

Mass spectra were also collected for electrosprays running at the minimum flowrates of the original source, as specified in Table 3. The process of collecting and integrating the mass spectra for each flowrate is described by Terhune et al.[37] The integrated spectra of the neat IL electrospray operating at the minimum flowrate, with and without an applied magnetic field, is show in Figure 5, while the integrated spectra for ILFF-10 and ILFF-30, with and without an applied magnetic field are provided in Figure 6. In both Figure 5 and 6, the lower range of masses are shown in the main plot. The spectra of both flowrates have been normalized such that the n = 0 peak equals an arbitrary intensity of 1e5, spectrum obtained with the 200-Gauss magnetic field shifted on the m/q axis by 20 amu/e. The inset plot shows the larger m/q range illustrating the larger mass distributions of the electrospray beam. Cations species within the spectra are denoted as n = 0, n = 1, and n = 2 for $EMIM^+$, [EMIM-NTf2] $EMIM^+$, and $[EMIM\text{-}NTf2]_2$ $EMIM^+$, respectively.

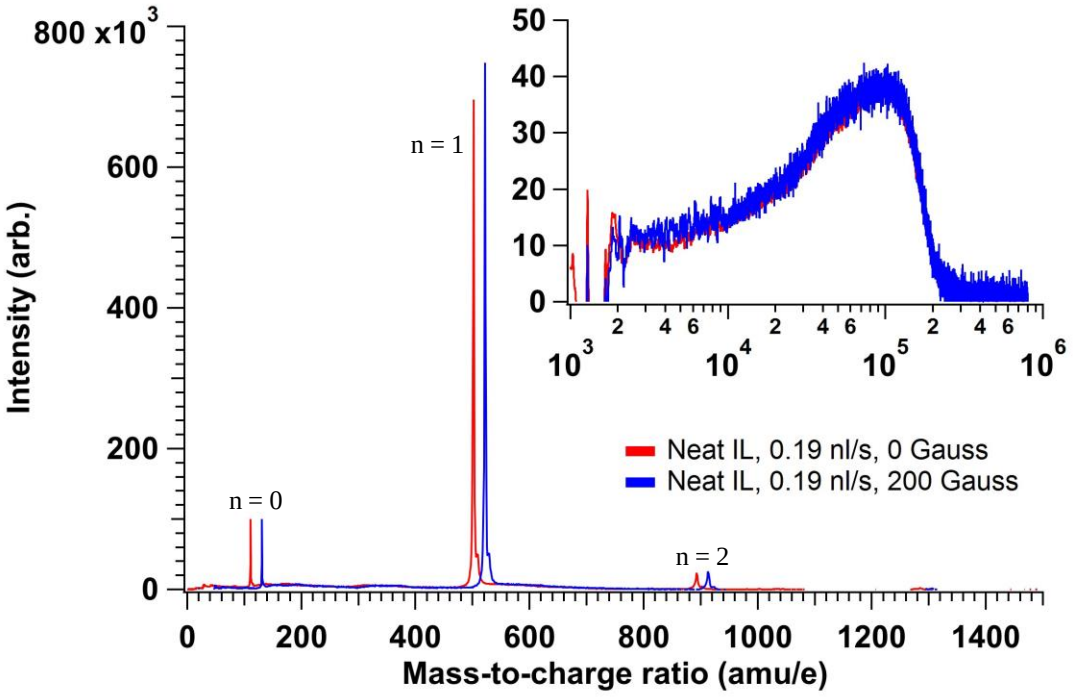

Figure 6. Mass spectra neat IL emitted from the capillary source at its minimum flowrate under zero and 200-Gauss applied magnetic fields. The spectra in the low-mass plot (0-1500 amu/e) have been incrementally shifted by 20 amu/e to ease comparison.

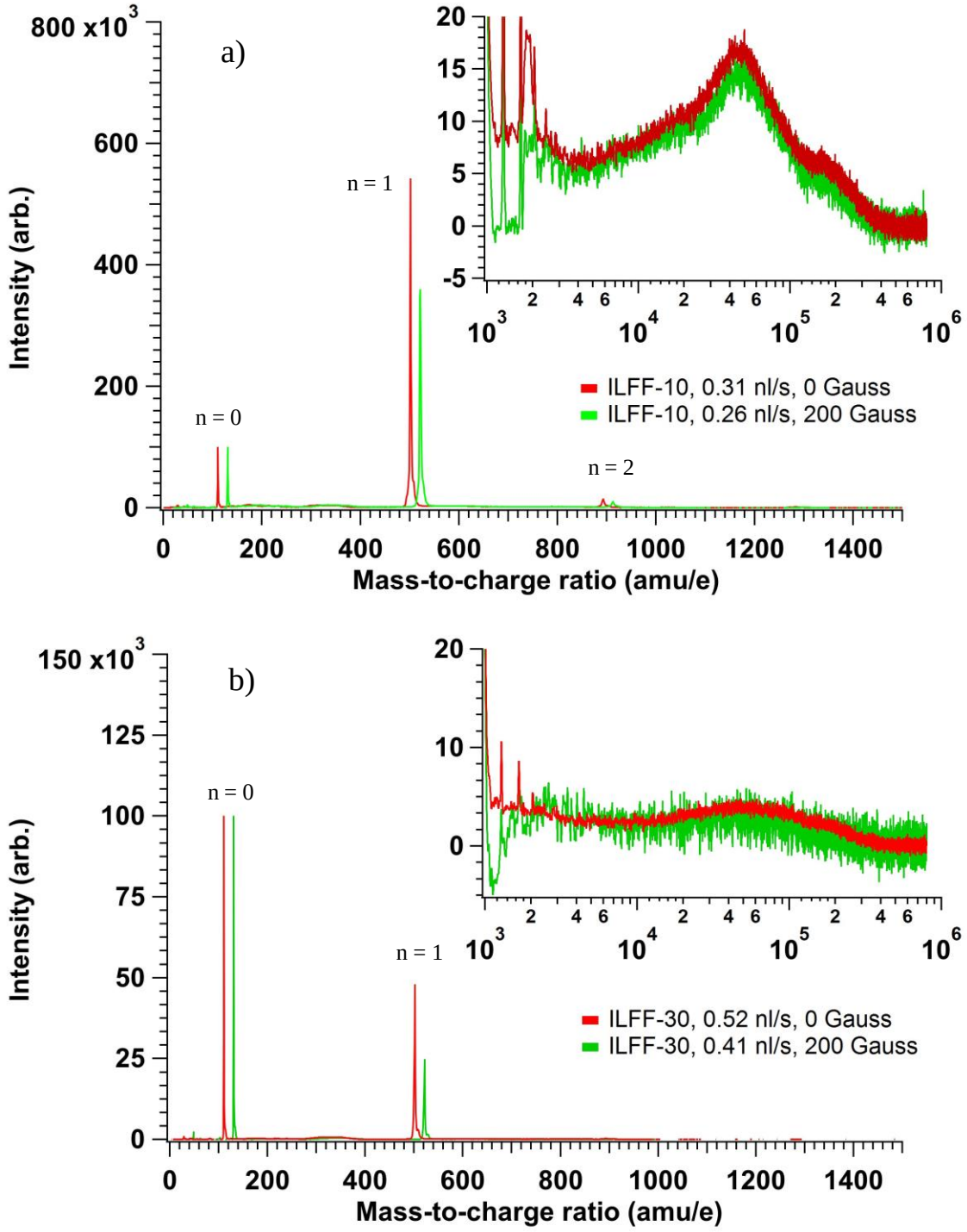

Figure 7. (a) Mass spectra of ILFF-10 solution emitted from the capillary source at its minimum flowrate under zero and 200-Gauss applied magnetic fields. (b) Mass spectra of ILFF-30 solution emitted from the capillary source at its minimum flowrate under zero and 200-Gauss applied magnetic fields. The spectra in the low-mass plot (0-1500 amu/e) have been incrementally shifted by 20 amu/e to ease comparison.

VI. Discussion

A. Effects of Nanoparticle Concentration

The nanoparticles have a measurable effect on the operational range of electrospray emission, as illustrated by Table 3. The extraction voltages required for stable electrospray needed to be increased up to 500 V between the neat IL and ILFF-10, and the ILFF-30 and ILFF-50 solutions. Furthermore, the minimum stable flowrate of the ILFF-10, ILFF-30 and ILFF-50 solutions significantly increased compared to the minimum flowrate of the neat IL. The increase in minimum flowrate was not linearly propotional to the concentration of nanoparticles in the neat IL; however, the two solutions with larger wt% of nanoparticles had significantly higher minimum flowrates than the neat IL of ILFF-10 suggesting a correlation to nanoparticle concentration.

The nanoparticles also changed the viscosity of the fluid. The viscosity of the parent ILFF was previously reported to have similar viscosities as the neat IL.[38] However, measured values for the vial pressure required to produce the same volumetric flowrate using different ILFF solutions, shown in Table 2, suggests that this is not correct. Fluid viscosity can be calculated from the Hagen- Poiseuille equation given a known flow rate, supply pressure, and feed-tube geometry as shown Equation 4.

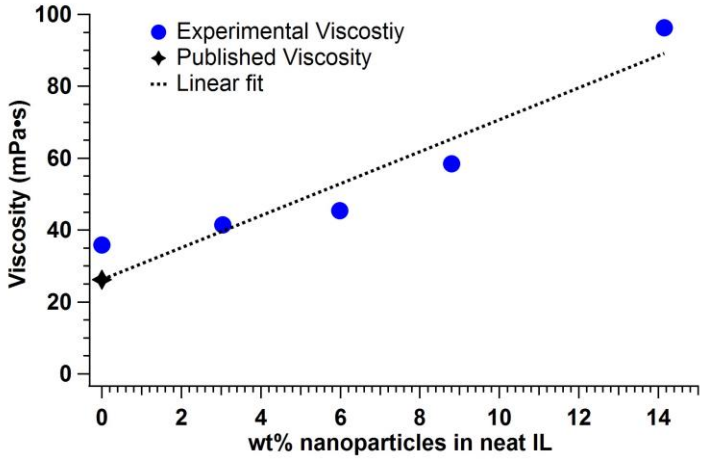

Figure 8. Viscosity of ILFF solutions based on the weight percent of nanoparticles in each solution. The published viscosity of neat EMIM-NTf2 is also plotted and used as the zero of the linear fit.

$$\eta = \frac{\Delta P \pi r_c^{\,4}}{8 L_c Q} \tag{4}$$

Figure 8 shows the values of viscosity for each ILFF solution determined using Eq. 4; also plotted is the published viscosity of neat EMIM-NTf2.[39] The addition of 14 wt% of nanoparticles approximately triples the viscosity of the neat IL, which may affect electrospray emission of the ILFF solution even when operating at the same flowrate.

The nanoparticles also had a significant effect on the emission current from the source. The emission current from a capillary electrospray source has been well established to depend upon surface tension, γ, conductivity, K, and flowrate, Q according to Eq. 1.[1,40-44] The emission currents for neat IL electrospray reported in Table 2 are comparable with other published emission current of neat EMIM-NTf2 electrosprays operating at similar flowrates; *e.g.* Gamero-Castaño reported absolute emission currents of 420, 490, and 573 nA for EMIM-NTf2 capillary electrosprays running at 0.52, 0.75 and 1.1 nl/s.[45] Emitted current from capillary sources operating on other ionic liquids that have different liquid and electrical properties also follow Eq. 1; e.g. Miller et al. reported absolute emission currents of a 1-butyl-3-methylimidazolium dicyanamide (BMIM-DCA) capillary electrospray at 589, 772, and 1032 nA for flowrates 0.46, 0.82, 1.29 nl/s.[7] The increase in BMIM-DCA emission current compared to EMIM-NTf2 at similar flowrates is the result of the increase in conductivity, from 0.92 to 1.052 S/m, surface tension, from 35.7 mN/m to 48.6 mN/m, and a decrease in electrical permittivity, from 12.3 to 11.3. The ILFF solutions used in Exp-1 and Exp-2 also have different fluid and electrical properties than its neat IL carrier fluid. These changes in properties are expected to affect the emission current relative to the carrier neat IL in accordance with Eq. 1.

The parent ILFF used to create the ILFF solutions has a conductivity of 0.57 S/m and surface tension of 32.39 mN/m, compared to 0.91 S/m and 36.28 mN/m, respectively, for the neat IL (permittivity was not measured). The properties of the diluted ILFF solutions were not measured, but it is reasonable to expect them to be a linear interpolation between that of the parent ILFF and the neat IL, as shown in Figure 9. Assuming linear properties for the ILFF solutions, a worthwhile comparison between the four electrosprays measured in this work (neat IL, ILFF-

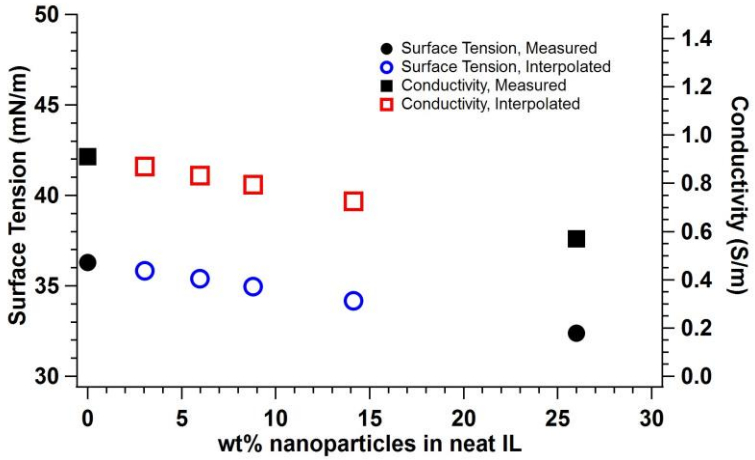

Figure 9. Measured surface tension and conductivity of neat IL and parent ILFF (black), and interpolated surface tension (blue) and conductivity (red) of IL as a function of wt% nanoparticles added to the neat liquid.

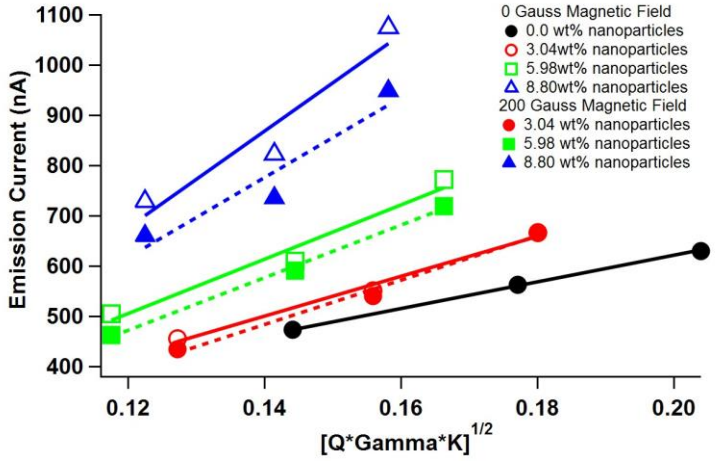

Figure 10. Measured emission current magnitude for electrosprays using neat IL and the three lower wt% ILFF solutions with zero magnetic field plotted against $\sqrt{\gamma KQ}$. Also shown are measured emission current magnitudes for electrosprays using the three lower wt% ILFF solutions with a 200-Gauss magnetic field. Linear fits for each electrospray with (hashed) and without magnetic field (solid) follow $I \sim \sqrt{\gamma KQ}$.

10, ILFF-20, and ILFF-30) is the emission current proportionality $I \sim \sqrt{\gamma KQ}$. The proportionality constant is the permittivity dependent de la Mora constant of Eq. 1[41] divided by the square-root of permittivity, $F(\varepsilon)/\varepsilon^{1/2}$. This relationship is plotted for neat IL, ILFF-10, ILFF-20, and ILFF-30 electrosprays operating without a magnetic field, and ILFF-10, ILFF-20, and ILFF-30 electrosprays operating with a 200-Gauss magnetic field in Figure 10. Emission currents from a neat IL electrospray with magnetic field were not measured for this source configuration, however, Figure 5 shows that the magnetic field has no influence on neat IL spray. As the concentration of nanoparticles increases so also does the slope of the *I* vs. $\sqrt{\gamma KQ}$ line. This suggests that either the permittivity of the neat IL has changed based on the amount of nanoparticles added to the liquid and/or some other mechanism of colloid electrosprays exists that affects the electrospray emission dynamics.

For a given concentration of nanoparticles, the slope of the *I* vs. $\sqrt{\gamma KQ}$ lines appear approximately the same for both zero and 200-G magnetic field, although the lines are shifted to lower values of current when the field is applied. This effect becomes more pronounced as the concentration of nanoparticles is increased. The permittivity of other magnetic fluids has been shown to vary depending on the magnetic field.[46] However, this effect has only been observed with micrometer-sized nanoparticles that form linear chains. The nanometer-scale particles used in our fluid are approximately spherical and are known to remain independent (no chains) even under application of a magnetic field.

Evidence that the nanoparticles affect the emission dynamics is reported in Terhune et al. where the ratio of light ions to large mass distributions emitted from a capillary electrospray source using the ILFF-10, ILFF-20, and ILFF-30 solutions increased with the addition of nanoparticles.[37] Due to the large difference in charge-to-mass between ion species and droplets, even a small shift in the fraction of the electrospray beam that is ions results in a large jump in emission current.

The influence that the nanoparticles have on the emitted species and/or jet dynamics may come from the size of the nanoparticles. The monodisperse particles have a diameter of 30 nm, whereas highly conductive electrosprays like those used in Exp-1, Exp-2 and Exp-3, have jet diameters of 26 to 49 nm for the range of flowrates used in these experiments.[45] Furthermore, as discussed by Terhune et al.[37] the estimated droplet diameter of neat IL with a charge of 40-percent the droplet's Rayleigh limit is on the order of 20 nm. Consequently, the nanoparticles must certainly influence the cone-jet formation and breakup. Specifically, Table 2 shows that ILFF-30 had a 90-percent increase in emission current when compared to the neat IL when both operating at approximately 0.90 nl/s. Given that the flowrate

is fixed the only conclusion is that the nanoparticles inhibited jet production, or invoked another phenomenon not known, that reduced the creation of larger masses and instead enabled the emission of a larger fraction of lighter particles, i.e. smaller m/q.

B. Effects of Magnetic Stress

The magnetic field affected the measured emission current of the electrospray as shown in both Table 2 and Figure 10. The effect of a 200-Gauss magnetic field acting on the electrospray, quantified as a percentage change in the emission current of the zero-magnetic-field electrospray, is shown in Figure 11. The effect is more significant for higher concentrations of nanoparticles; e.g. the emission current from an electrospray with 3.04 wt% nanoparticles was reduced by 0 to 4 percent of the zero-magnetic-field magnitude when a 200-Gauss magnetic field was applied, whereas the emission current from the electrospray with 8.80 wt% nanoparticles saw a greater reduction of 9 to 12 percent of the zero-magnetic-field magnitude.

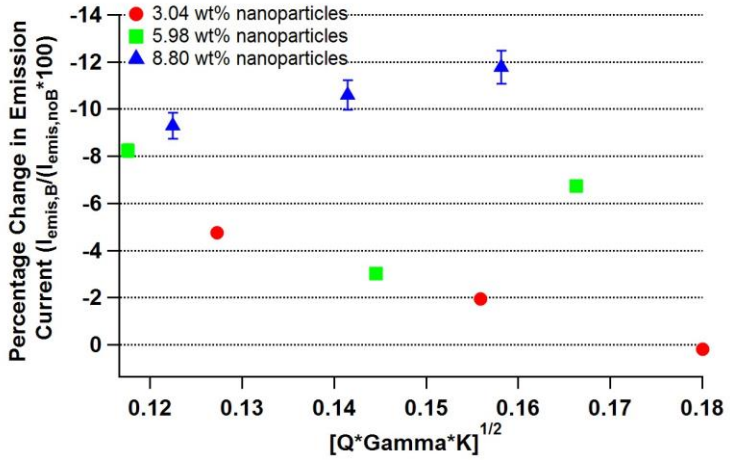

Figure 11. Percentage change in the emission current from a that of an electrospray in zero-magnetic-field plotted against the flowrate for electrosprays running ILFF-10, ILFF-20 and ILFF-30 solutions. Change caused by the application of a 200-Gauss magnetic field.

Also apparent throughout testing was the fluctuation in the emission current while the magnetic field was applied. This was accentuated with the increase in the nanoparticles in the neat IL. These fluctuations significantly affected the spray when the concentration of nanoparticles was above 30 wt%, i.e. ILFF-40 and ILFF-50. Specifically, the emission current of the electrospray during application of the magnetic field began to fluctuate by more than 10% and the fluctuations persisted for several minutes after removal of the field.

Correlation between the variability in the emission current from the electrosprays and the application of the magnetic field may be the product of the magnetic stress interacting with the emission site geometry. Perturbations, such as Taylor cones, on the surface of magnetic liquid are known to increase the gradient of the magnetic field (∇B).[22,30,47,48] This would lead to a higher magnetic field at the apex of the emitter and may change the mobility dynamics of the nanoparticles to, and/or the formation of the Taylor cone at the emission site. However, this mechanism is not fully understood, and whether it has significant effect on electrospray emission is uncertain, thus motivation exists for further investigation on the relative change in emission current while magnetically stressed.

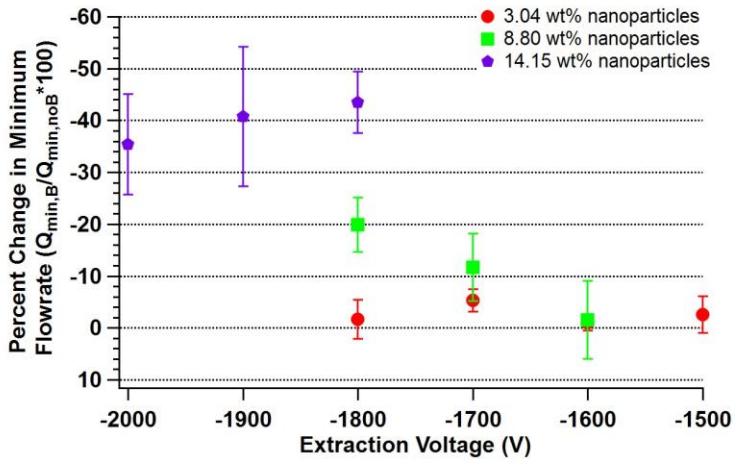

Figure 12. Percent change in the minimum flowrate from a zero-magnetic-field case for ILFF-10, ILFF-30, and ILFF-50 solution. Caused by the application of a 200-Gauss magnetic field.

The magnetic field also had a significant effect on the minimum stable flowrate of electrosprays running on the ILFF solutions. The results in Table 3 show that with only a small addition of ferromagnetic nanoparticles, 8.8 wt%, it is possible to reduce the minimum flowrate for stable emission by applying a magnetic field.; the reduction was 15-percent of the minimum flowrate of the same electrospray operating with zero magnetic field. Furthermore, the results show a correlation between the nanoparticle concentration and the reduction in the minimum flowrate caused by a magnetic stress, with a 43 ± 6-percent reduction using ILFF-50 solution (14.15 wt% nanoparticles) at an extraction voltage of -1800 V (Figure 8) compared to the same

solution operating in a zero magnetic field. By reducing the flowrate of the electrospray, the emitted species are also effected, as seen in Figure 6. The ratio of n = 1 to n = 0 is reduced by 33- to 50-percent depending on the solution, which is significant even with a 20-percent uncertainty in intensity axis (see section VI A. in Terhune et al.[37] for description regarding spectra comparison and repeatability). This is interpreted as a shift in the average m/q from heavier to lighter mass species. As this relates to propulsion, this states that the application of a magnetic field would provide higher specific impulse for a given fluid. Note that, as observed in Figure 5, the field had no significant effect on the neat IL minimum flowrate.

Madden et al. observed similar effects in their work with low-conductivity ferrofluids.[31] In their work two sulfolane ferrofluid solutions were used, one with 15% (v/v) ethyl ammonium nitrate (EAN), and the other with 0.1% (v/v) EAN. With the application of a 300-Gauss magnetic field they saw a significant expansion of the operational range of the electrospray. Specifically, a 40-percent and 30-percent drop in minimum flowrate for the 15% EAN and 0.1% EAN solutions, respectively. Furthermore, the minimum voltage at which a Taylor cone formed was reduced by 23-percent and 24-percent for the 15% EAN and 0.1% EAN solutions, respectively.

Conclusion

The emission current and minimum flowrate was measured for a capillary electrospray source operating on a neat IL propellant and four solutions of an ILFF propellant. Furthermore, the beam emitted from the capillary source operating at the minimum flowrate was measured using a TOF mass spectrometer. The parent ILFF was comprised of 26.0 wt% iron oxide nanoparticles, 4.6 wt% copolymer, and 69.4 wt% EMIM-NTf2. The solutions of ILFF were produced by adding 10, 20, 30 and 50 % (v/v) to the neat IL which resulted in nanoparticle concentrations of 3.04, 5.98, 8.80, and 14.15 wt%, respectively. The emission current and minimum flowrate was measured for the same capillary source, running on the same five propellants, while subjected to a 200-Gauss magnetic field concentrically aligned with the capillary needle; the resulting beam while operating at the minimum flowrate was also measured using a TOF mass spectrometer. The magnetic field was produced using a Helmholtz coil to create a gradient-free field within its the hollow core. The resulting mass spectra were shown to be dependent on two new variables, the nanoparticle concentration and the applied magnetic field.

The emission current of the electrospray correlated to the concentration of nanoparticles, with the emission current significantly increasing (compared to the emission current of the neat IL operating at the same conditions) when the amount of nanoparticles within the electrosprayed propellant was increased. The emission current follows the trend of $I \sim \sqrt{\gamma K Q}$, albeit with a slope that depends upon the nanoparticle concentration. This suggest that the permittivity of the ILFF solutions is different from the neat IL. Furthermore, the nanoparticle concentration increases the viscosity of the neat IL, which could also affect the emission dynamics of the spray.

The emission current also had a correlation with the magnetic field; an application of 200 Gauss to an operating electrospray decreased the emission current by 10 to 12 percent for an ILFF solution with 8.80 wt% nanoparticles (compared to the emission current of the neat IL operating at the same conditions). Extended operation of the two ILFF solutions with higher than 8.80 wt% resulted in fluctuations of the emission current that remain for several minutes after the removal of the field.

The minimum flowrate for stable operation of the electrospray operating on the ILFF solutions was reduced through the application of the 200-Gauss magnetic field. The percentage of flowrate reduction was dependent on the amount of nanoparticles in the solution with a maximum of 43 percent reduction compared to the zero-magnetic-field-minimum flowrate, when using a solution with 14.15 wt% nanoparticles. The reduction of the minimum flowrate aligns with studies on low-conductivity Sulfolane ferrofluids,[31] and should be further investigated to realize the interaction mechanism between the magnetic field and the high-conductivity ferrofluids.

Acknowledgments

KJT would like to thank Marty Toth and Bill Langdon for machining all custom components for the experiments. All the authors would like to thank the Air Force Research Lab at Kirtland AFB for providing the facilities to conduct the testing. They would also like to thank the US Air Force Office of Scientific Research: International AOARD and Sirtex Medical Limited for funding the development of the ILFFs, and Steve Jones and Stephanie Bickley for designing and preparing the monodomain magnetic particles. The material is based upon work supported by NASA under award No NNX13AM73H. Any opinions, findings, and conclusions or recommendations expressed in this material are those of the authors and do not necessarily reflect the views of the National Aeronautics and Space Administration. BDP acknowledges support from the Air Force Office of Scientific Research under task number 16RVCOR275 (Program Manager: Michael Berman).

References

1. Fernández de la Mora, J., "The Fluid Dynamics of Taylor Cones," Annual Review of Fluid Mechanics, 39, 2006, pp. 217-243
2. Fernández de la Mora, J., et al., "Electrochemical processes in electrospray ionization mass spectrometry," Journal of Mass Spectrometry, 35, 2000, pp. 939-952
3. Shevchenko, A., M. Wilm, O. Vorm, and M. Mann, "Mass spectrometric sequencing of proteins silver-stained polyacrylamide gels," Anal Chem, 68, 1996, pp. 850-8
4. Jackson, G.P. and D.C. Duckworth, "Electrospray mass spectrometry of undiluted ionic liquids," Chemical Communications, 0, 2004, pp. 522-523
5. Chiu, Y.H., et al., "Vacuum electrospray ionization study of the ionic liquid, [Emim][Im]," International Journal of Mass Spectrometry, 265, 2007, pp. 146-158
6. Miller, S.W., B.D. Prince, and J.L. Rovey, "Capillary Extraction of the Ionic Liquid [Bmim][DCA] for Variable Flow Rate Operations," *48th AIAA/ASME/SAE/ASEE Joint Propulsion Conference & Exhibit*, Atlanta, Georgia, 30 July - 1 August 2012
7. Miller, S.W., B.D. Prince, R.J. Bemish, and J.L. Rovey, "Electrospray of 1-Butyl-3-Methylimidazolium Dicyanamide Under Variable Flow Rate Operations," Journal of Propulsion and Power, 2014, pp. 1-10
8. Doshi, J. and D.H. Reneker, "Electrospinning process and applications of electrospun fibers," *Industry Applications Society Annual Meeting, 1993., Conference Record of the 1993 IEEE,* 2-8 Oct 1993
9. Yarin, A.L., S. Koombhongse, and D.H. Reneker, "Taylor cone and jetting from liquid droplets in electrospinning of nanofibers," Journal of Applied Physics, 90, 2001, pp. 4836-4846
10. Morozov, V.N. and T.Y. Morozova, "Electrospray Deposition as a Method for Mass Fabrication of Mono- and Multicomponent Microarrays of Biological and Biologically Active Substances," Analytical Chemistry, 71, 1999, pp. 3110-3117
11. Uematsu, I., et al., "Surface morphology and biological activity of protein thin films produced by electrospray deposition," Journal of Colloid and Interface Science, 269, 2004, pp. 336-340
12. Oh, H., K. Kim, and S. Kim, "Characterization of deposition patterns produced by twin-nozzle electrospray," Journal of Aerosol Science, 39, 2008, pp. 801-813
13. Gamero-Castaño, M. and V. Hruby, "Electrospray as a Source of Nanoparticles for Efficient Colloid Thrusters," Journal of Propulsion and Power, 17, 2001, pp. 977-987
14. Lozano, P.C., "Studies on the Ion-Droplet Mixed Regime in Colloid Thrusters," Department of Aeronautics and Astronautics, Massachusetts Institute of Technology, 2003
15. Ziemer, J.K., "Performance of Electrospray Thrusters," *31st International Electric Propulsion Conference,* Ann Arbor, Michigan,
16. Martel, F., L. Perna, and P. Lozano, "Miniature Ion Electrospray Thrusters and Performance Tests on Cubesats," *Proceedings of the AIAA/USU Conference on Small Satellites,* 2012
17. MacFarlane, D.R., S.A. Forsyth, J. Golding, and G.B. Deacon, "Ionic liquids based on imidazolium, ammonium and pyrrolidinium salts of the dicyanamide anion," Green Chemistry, 4, 2002, pp. 444-448
18. Baker, G.A., S.N. Baker, S. Pandey, and F.V. Bright, "An analytical view of ionic liquids," Analyst, 130, 2005, pp. 800-808
19. Prince, B.D., B.A. Fritz, and Y.-H. Chiu, *Ionic Liquids in Electrospray Propulsion Systems*, in *Ionic Liquids: Science and Applications*2012, American Chemical Society. p. 27-49.
20. Meyer, E.J., Lyon B. King, Nirmesh Jain, and Brian S. Hawkett, " Ionic liquid ferrofluid electrospray with EMIM-NTf2 and ferrofluid mode studies with FerroTec EFH-1 in a non-uniform magnetic field " *33rd International Electric Propulsion Conference* The George Washington University, USA, 6 -10 October 2013
21. Meyer, E.J., Lyon B. King, "Electrospray from an Ionic Liquid Ferrofluid utilizing the Rosensweig Instability " *49th AIAA/ASME/SAE/ASEE Joint Propulsion Conference & Exhibit,* San Jose, CA, 14-17 July 2013
22. King, L.B., et al., "Self-Assembling Array of Magnetoelectrostatic Jets from the Surface of a Superparamagnetic Ionic Liquid," Langmuir, 30, 2014, pp. 14143-14150
23. Jackson, B.A., "Characterization of an Ionic Liquid Ferrofluid Electrospray Emission Pattern," *50th AIAA/ASME/SAE/ASEE Joint Propulsion Conference & Exhibit,* Cleveland, OH, 28-30 July 2014
24. King, L.B., "Ferroelectrohydrodynamics of ionic liquid ferrofluid surface instabilities and jets," *50th AIAA/ASME/SAE/ASEE Joint Propulsion Conference & Exhibit,* Cleveland, OH, 28-30 July 2014
25. Lozano, P. and M. Martínez-Sánchez, "On the dynamic response of externally wetted ionic liquid ion sources," Journal of Physics D: Applied Physics, 38, 2005, pp. 2371
26. Lozano, P. and M. Martínez-Sánchez, "Ionic liquid ion sources: suppression of electrochemical reactions using voltage alternation," Journal of Colloid and Interface Science, 280, 2004, pp. 149-154
27. Chiu, Y.-H., et al., "Mass Spectrometric Analysis of Ion Emission for Selected Colloid Thruster Fuels," *39th AIAA/ASME/SAE/ASEE Joint Propulsion Conference and Exhibit,* Huntsville, Alabama,
28. Jain, N., et al., "Optimized steric stabilization of aqueous ferrofluids and magnetic nanoparticles," Langmuir, 2009, pp.
29. Jain, N., X. Zhang, B.S. Hawkett, and G.G. Warr, "Stable and Water-Tolerant Ionic Liquid Ferrofluids," ACS Applied Materials & Interfaces, 3, 2011, pp. 662-667
30. Rosensweig, R.E., *Ferrohydrodynamics* 1985, Mineola: Dover Publications, Inc.
31. Madden, A., J. Fernández de la Mora, B. Hawkett, and N. Jain, "Effect of a homogeneous magnetic field on the electrospraying characteristics of sulfolane ferrofluids," *Unpublished Manuscript*, Yale University, 2016

32. Terhune, K.J., Lyon B. King, Michael L. Hause, Benjamin D. Prince, Nirmesh Jain, Brian S. Hawkett, "Species measurements in the beam of an ionic liquid ferrofluid electrospray source," *50th AIAA/ASME/SAE/ASEE Joint Propulsion Conference & Exhibit*, Cleveland, OH, 28-30 July 2014
33. Krpoun, R. and H.R. Shea, "Integrated out-of-plane nanoelectrospray thruster arrays for spacecraft propulsion," Journal of Micromechanics and Microengineering, 19, 2009, pp. 045019
34. Chiu, Y.-H., et al., "Mass Spectrometric Analysis of Colloid Thruster Ion Emission from Selected Propellants," Journal of Propulsion and Power, 21, 2005, pp. 416-423
35. Romero-Sanz, I., R. Bocanegra, J.F. de la Mora, and M. Gamero-Castano, "Source of heavy molecular ions based on Taylor cones of ionic liquids operating in the pure ion evaporation regime," Journal of Applied Physics, 94, 2003, pp. 3599-3605
36. Miller, S.W., B.D. Prince, R.J. Bemish, and J.L. Rovey, "Mass Spectrometry of Selected Ionic Liquids in Capillary Electrospray at Nanoliter Volumetric Flow Rates," *52nd AIAA/SAE/ASEE Joint Propulsion Conference*, Salt Lake City, UT, 25-27 July 2016
37. Terhune, K.J., Lyon B. King, Benjamin D. Prince, Nirmesh Jain, Brian S. Hawkett, "Species measurements in the beam of an ionic liquid ferrofluid capillary electrospray source under magnetic stress," *52nd AIAA/SAE/ASEE Joint Propulsion Conference*, Salt Lake City, UT, 25-27 July 2016
38. Meyer IV, E.J., "Development of an Ionic Liquid Ferrofluid Electrospray Source and Mode Shape Studies of a Ferrofluid in a Non-uniform Magnetic Field," *Doctoral Dissertation*, Mechanical Engineering - Engineering Mechanics, Michigan Technological University, 2014
39. Fröba, A.P., H. Kremer, and A. Leipertz, "Density, Refractive Index, Interfacial Tension, and Viscosity of Ionic Liquids [EMIM][EtSO4], [EMIM][NTf2], [EMIM][N(CN)2], and [OMA][NTf2] in Dependence on Temperature at Atmospheric Pressure," The Journal of Physical Chemistry B, 112, 2008, pp. 12420-12430
40. Higuera, F.J., "Flow rate and electric current emitted by a Taylor cone," Journal of Fluid Mechanics, 484, 2003, pp. 303-327
41. Fernández de la Mora, J. and I.G. Loscertales, "The current emitted by highly conducting Taylor cones," Journal of Fluid Mechanics, 260, 1994, pp. 155-184
42. Garoz, D., et al., "Taylor cones of ionic liquids from capillary tubes as sources of pure ions: The role of surface tension and electrical conductivity," Journal of Applied Physics, 102, 2007, pp. 064913-10
43. Gamero-Castaño, M. and J. Fernández de la Mora, "Direct measurement of ion evaporation kinetics from electrified liquid surfaces," The Journal of Chemical Physics, 113, 2000, pp. 815-832
44. Gañán-Calvo, A.M., "On the theory of electrohydrodynamically driven capillary jets," Journal of Fluid Mechanics, 335, 1997, pp. 165-188
45. Gamero-Castaño, M., "Characterization of the electrosprays of 1-ethyl-3-methylimidazolium bis(trifluoromethylsulfonyl) imide in vacuum," Physics of Fluids, 20, 2008, pp. 032103
46. Polcar, P. and D. Mayer, "Magnetic Field Controlled Capacitor," Journal of Electrical Engineering, 67, 2016, pp. 227-230
47. Rosensweig, R.E., "Magnetic Fluids," Annual Review of Fluid Mechanics, 19, 1987, pp. 437-461
48. Boudouvis, A.G., J.L. Puchalla, L.E. Scriven, and R.E. Rosensweig, "Normal field instability and patterns in pools of ferrofluid," Journal of Magnetism and Magnetic Materials, 65, 1987, pp. 307-310